Journal of Hydro-environment Research 54 (2024) 26–36

Contents lists available at ScienceDirect

Journal of Hydro-environment Research

journal homepage: www.elsevier.com/locate/jher

# Self-aeration on large dam spillways during major floods

Hubert Chanson

*The University of Queensland, School of Civil Engineering, Brisbane, QLD 4072, Australia*

ARTICLE INFO

*Keywords:*
Self-aeration
Hydraulic structures
Spillways
Field observations
Major floods

ABSTRACT

In a spillway chute flow, the upstream flow is typically non-aerated and the flow becomes self-aerated when the turbulent stresses acting next to the water surface exceeds the combined resistance of gravity and surface tension. The inception region of air entrainment is a rapidly-varied region characterised by the transition from a monophase water to two-phase air–water flow. In this contribution, field observations were conducted at large dam spillways during major flood events, with a focus on prototype data for discharges between 100 $m^3/s$ and 6,000 $m^3/s$ and Reynolds numbers between $2.6 \times 10^6$ to $1.1 \times 10^8$. The onset of self-aeration was a complicated three-dimensional transient process, and the dimensionless location of the inception region was a function of the Reynolds number. Surface velocities obtained with an optical technique showed that the streamwise surface velocities were close to theoretical estimates, and the streamwise surface turbulent intensities in excess of 100 %, consistent with self-aerated measurements in laboratory. The current findings yield a couple of seminal questions: (a) what do we know about prototype spillway operation during major floods? (b) how large the Reynolds number of a prototype flow needs to be truly representative of large dam spillway self-aerated flows during major flood events?

## 1. Presentation

Dams and reservoirs constitute an efficient means to provide the society with both water security and flood protection (ICOLD, 1984). The dams are equipped with a spillway system designed to pass safely the flood waters during large rainfall events and major floods (USBR, 1965, Novak et al., 1996). Free-surface spillways with un-controlled crest are the "*safest*" design (Cassidy and Elder, 1984). In a free-surface chute flow, the upstream region is typically a non-aerated flow while some strong air–water mix occurs when the turbulent shear stress acting next to the free-surface exceeds the combined resistance of gravity and surface tension (Ervine and Falvey, 1987, Chanson, 2009). At the upstream end of a spillway, the flow is relatively rapidly accelerated and a turbulent boundary layer develops along the channel invert. On flat chutes, the onset region of self-aeration presents a transition from smooth to rough interface with free-surface instabilities (Michels and Lovely, 1953, Chanson, 1997) (Fig. 1A). It is thought that the inception of air entrainment is caused by a combination of longitudinal vortices' breakdown and of gravity waves produced by roughness and irregularities at the channel boundaries (Levi, 1965,1967, Anwar, 1994). On steep chutes, the inception of air entrainment is observed when the outer edge of the developing turbulent boundary layer starts interacting with the water surface (Rao and Rajaratnam, 1961, Hino, 1961). The interactions between the free-surface and boundary layer turbulence are very energetic and strong air–water ejections may be observed (Chanson, 2013,2022, Zabaleta and Bombardelli, 2020) (Fig. 1B & 1C). Despite some key differences, the two theories do not exclude each other, and this was discussed by Toro et al. (2017) and Chanson (2022). Typical examples of self-aeration processes are presented in Fig. 1, with a series of prototype chute operations illustrated with high-shutter speed photographs.

The performances of spillways are often investigated in physical and laboratory models, and the upscaling can be challenging (Elder 1984a, Kolkman, 1984). Hydraulic models can be un-necessarily expensive and unsatisfactory, whether a physical or numerical approach is selected. Late Professor Pavel Novak and his co-workers stressed that "*Field (prototype) measurements are of paramount importance, and are really the only way to confirm the validity of the conclusions drawn from the modelling process*" (Novak et al., 2010,p. 581). With large dam spillways, the spillway is designed for extreme events, i.e. major floods, but the personal experience and quantitative observations of their performance under these severe conditions is limited.

This contribution aims to discuss the inception processes of air entrainment in prototype dam spillways operating during major floods, with a focus on flow conditions for discharges between 100 $m^3/s$ and 6,000 $m^3/s$ and Reynolds numbers between $2.6 \times 10^6$ to $1.1 \times 10^8$. The

*E-mail address:* h.chanson@uq.edu.au.

https://doi.org/10.1016/j.jher.2024.03.002
Received 28 August 2023; Received in revised form 17 February 2024; Accepted 15 March 2024
Available online 16 March 2024

prototype observations were undertaken a three sites in eastern Australia. Some key features of the onset of self-aeration are described and detailed observations of surface velocity fields are discussed.

## 2. Field observations at prototype spillways

The prototype observations were conducted at three large dam spillways in eastern Australia, between 2010 and 2022 (Fig. 2). The three structures were the Paradise Dam, the Hinze Dam, and the Chinchilla Weir (Table 1). Table 1 summarises the spillway flow conditions during the observations, including the Reynolds number Re being defined in terms of the equivalent pipe diameter. All the three hydraulic structures are listed as large dams by the Australian committee on large dams (ANCOLD) and the international committee on large dams (ICOLD).

The Paradise dam is a roller compacted concrete (RCC) structure located along the Burnett River and equipped with a 315 m wide primary stepped spillway and an un-controlled ogee crest. The final chute slope is $\theta = 57.38°$ (i.e. 1V:0.64H) and the steps are 0.62 m high. Photographic observations were undertaken from the right bank of the Burnett River in 2010 and 2013 (Fig. 3A).

The Hinze dam spillway is a steep stepped chute, followed by an energy dissipator located about 35 m below the chute crest. The final chute slope is $\theta = 51.3°$ (1V:0.8H) with 1.5 m high steps (Fig. 3B). The low section is designed to contain the 1:100 AEP flood event and it is 12.25 m wide (Chanson, 2022). Photographic and cinematographic

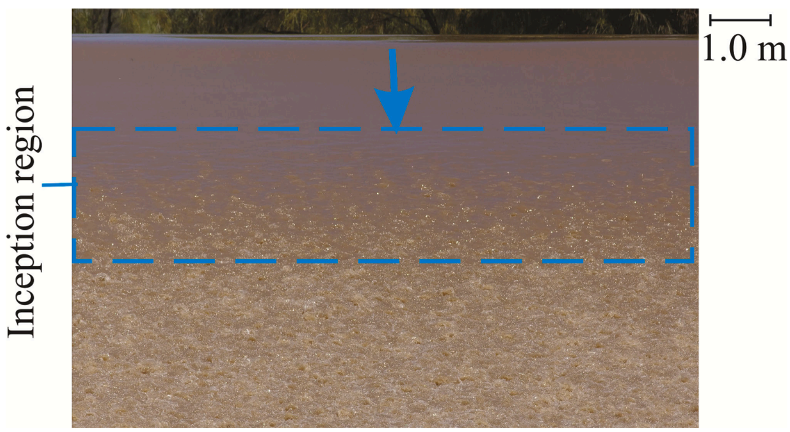


(A) High-shutter speed photograph of flat smooth chute spillway: Chinchilla weir, 15 December 2021, Q = 141 m$^3$/s, Re = $2.7 \times 10^6$ to $4.6 \times 10^6$, shutter speed: 1/2,000 s

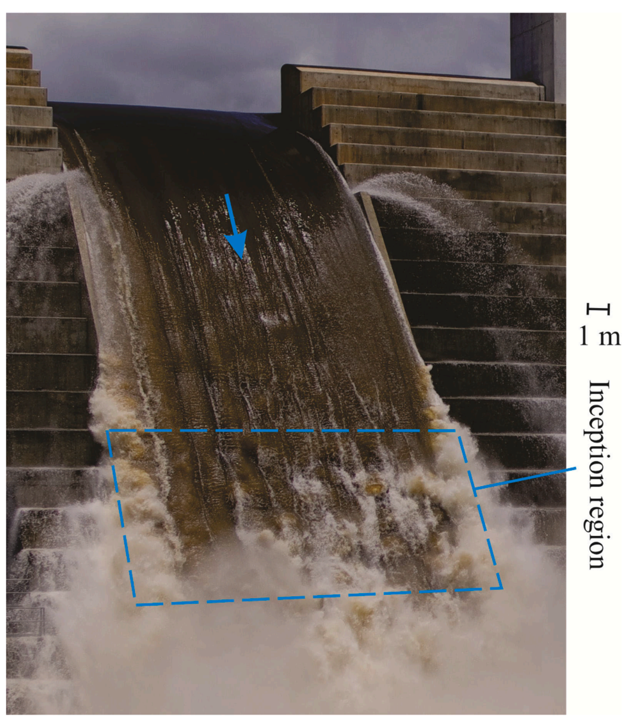


(B) High-shutter speed photograph of steep spillway chute: Hinze dam on 29 January 2013, Q = 202 m$^3$/s, Re = $6.7 \times 10^7$, shutter speed: 1/8,000 s

**Fig. 1.** Self-aeration in free-surface chute flows on prototype spillways.

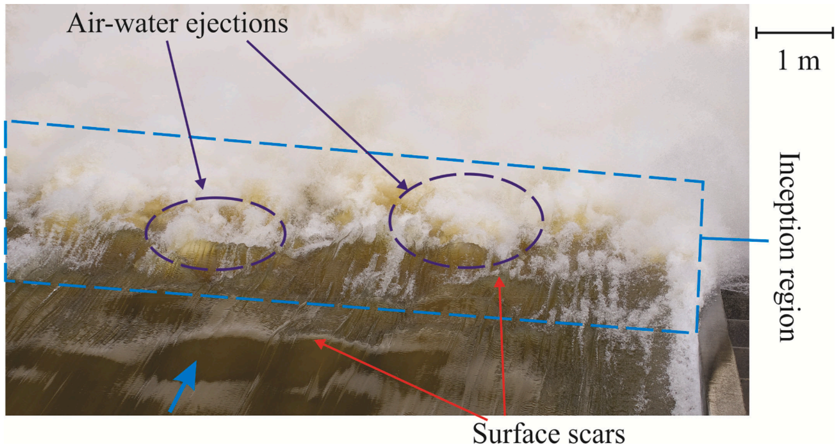


(C) High-shutter speed photograph of steep spillway chute: Hinze dam on 4 March 2022, Q = 111 $m^3/s$, Re = $3.6 \times 10^7$, shutter speed: 1/2,000 s

**Fig. 1.** (*continued*).


**Fig. 2.** Sketch of the location of the three large dam spillway.

records were conducted from two reinforced concrete platforms, located downstream of the spillway and directly above the chute crest, between 2010 and 2022.

The Chinchilla Weir is located on the Condamine River. The structure is a 14 m high earthfill embankment, with an overflow spillway channel. The chute consists of a broad crest, followed by a 60.6 m long smooth converging channel with a constant slope $\theta = 11.3°$ (1V:5H) (Fig. 3C). The chute convergence ratio is 2.18 m/m. The overflow chute is made of concrete slabs (Turnbull and McKay, 1974). The observations were performed from the right bank and from downstream, facing the left spillway bay in 2021 (Chanson and Apelt, 2022,2023).

Visual, photographic and cinematographic data were collected during a number of major flood events (Table 1). The observations were documented using dSLR cameras Pentax™ K-7, Pentax™ K-01 and Pentax™ K-3 with sensor resolutions ranging from 12 Mpx to 24 Mpx. These were complemented by records using digital cameras Casio™ EX10 Exilim and Sony™ RC100VA, and an Apple™ iPhone XI. The dSLR cameras were equipped with several full-frame prime lenses producing photographs and movies with negligible barrel distortion, and two zoom lenses. The latters were used mostly for qualitative and limited quantitative observations. The dSLR camera movies were recorded in high definition (1920 × 1080 px) at 30 fps and 60 fps, while the movies with the Casio™ and Sony™ cameras were recorded at 120 fps and 100 fps.

The analyses of free-surface features, including air–water structures, were performed based upon high-shutter speed photographs and movies. All the tracking and measurements of free-surface features were undertaken manually to maximise the quality control, owing to the

**Table 1**
Prototype spillway observations in eastern Australia (Present study).

| Spillway | Chute design | θ (°) | Date | Q ($m^3/s$) | q ($m^2/s$) | Re | Comments |
|---|---|---|---|---|---|---|---|
| Paradise dam | Stepped | 57.4 | 30/12/2010 | 5,965 | 18.9 | $7.5 \times 10^7$ | |
| | | | 5/03/2013 | 2,316 | 7.4 | $2.9 \times 10^7$ | |
| Hinze dam | Stepped | 51.3 | 29/01/2013 | 202 | 16.5 | $6.5 \times 10^7$ | See Chanson (2013) |
| | | | 3/05/2015 | 21 | 1.7 | $6.8 \times 10^6$ | |
| | | | 31/03/2017 | 334 | 27.3 | $1.1 \times 10^8$ | 1:100 AEP flood |
| | | | 23/03/2021 | 111 | 9.1 | $3.6 \times 10^7$ | |
| | | | 24/03/2021 | 140 | 11.4 | $4.5 \times 10^7$ | |
| | | | 27/03/2021 | 72 | 5.9 | $2.3 \times 10^7$ | |
| | | | 25/02/2022 | 52 | 4.3 | $1.7 \times 10^7$ | |
| | | | 27/02/2022 | 116 | 9.5 | $3.8 \times 10^7$ | |
| | | | 1/03/2022 | 249 | 20.4 | $8.1 \times 10^7$ | |
| | | | 3/03/2022 | 143 | 11.7 | $4.6 \times 10^7$ | |
| | | | 4/03/2022 | 111 | 9.1 | $3.6 \times 10^7$ | |
| | | | 5/03/2022 | 86 | 7.0 | $2.8 \times 10^7$ | |
| Chinchilla weir | Smooth | 11.3 | 27/11/2021 | 121 | 0.57 ([1]) | $2.3 \times 10^6$ ([1]) | |
| | | | 15/12/2021 | 144 | 0.67 ([1]) | $2.7 \times 10^6$ ([1]) | |

*Note*: ([1]) at the spillway crest.

complexity of the prototype turbulent flow motion. The prototype spillway flows were characterised by extremely rapid, quasi-random and large changes with time and space. Furthermore, a number of movies were processed using an optical flow (OF) technique, with the camera fixed on a sturdy tripod and equipped with full-frame prime lenses. The OF is a set of tools, detecting the flow motion between consecutive frames based upon brightness intensity changes, originally developed by computer vision scientists (Bung and Valero, 2016, Zhang and Chanson, 2019). In this study, the OF technique was based upon the Farneback method. The Farneback technique was applied using parameters previously obtained and validated in laboratory for surface velocity (Arosquipa Nina et al., 2022). The application to prototype spillway chutes was carefully validated against theoretical analyses and large-size physical model (Chanson, 2022, Chanson and Apelt, 2022).

## 3. Prototype spillway flow observations

### 3.1. Air-water flow features

For all flood events, the approach flow conditions were observed to be very smooth at all spillway structures. This was confirmed by aerial photographs and drone footages during a select number of events (Fig. 3A & Chanson, 2023). In the reservoir, the flow converged smoothly towards the spillway crest, and the upstream water surface was waveless and quasi-still. For all observation conditions (Table 1), the flow was critical at the un-controlled crest, acting as a hydraulic control. The smooth change on water surface elevation between the upstream reservoir and the upstream end of the chute was thoroughly documented with photographs, movies and aerial footage.

On the spillway chute, the flow accelerated and the water surface became rough and choppy, before becoming self-aerated. The inception region presented markedly different features between flat-slope and steep slope structures. On flat-slope chutes, a progressive transition of surface roughness was seen, as documented at Chinchilla weir in 1997, 2011, 2021 and 2022 (Chanson and Apelt, 2023), and at other flat-slope chute weirs (Anwar, 1994). Down un-controlled flat-slope chutes, the water surface roughness changed progressively from a glassy surface to a rough appearance, followed by a choppy wavy texture, becoming self-aerated, i.e. the inception region (Fig. 1A & 3C). The inception region corresponded to the progressive change in surface texture and roughness. Downstream of the inception region, the self-aerated chute flow at Chinchilla weir exhibited a beige colour, systematically documented in 1974, 1997, 2011, 2021 and 2022. The beige colour was evidence of the three-phase nature of the air–water-sediment motion (Chanson, 2013).

On steep spillway chutes, the inception region was characterised by a brutal transition from non-aerated to self-aerated flow, with explosive interactions between large-scale turbulent structures and the water surface (Fig. 1B, 1C, 3A, 3B, & 4A). Short-lived very-energetic surface scars and boils were observed immediately upstream of the onset of free-surface aeration. The surface scars initiated and developed primarily as transverse entities, although the generation process could include a mix of both longitudinal and transverse scar initiation (Chanson, 2022). Fig. 4B presents the dimensionless growth of the transverse width of air–water surface features in the vicinity of the onset region. The graphs regroups both prototype and laboratory data obtained with high-shutter speed records (Table 2). Details of the flow conditions are listed in Table 2, including the aspect ratio $B/d_c$, defined as the ratio of chute width B to critical depth $d_c$, and the camera frame rate in frames per second (fps). For all the data sets (Table 2), the growth of transverse cars was best correlated by

$$\frac{w}{d_c} = 0.888 \times \left( t \times \sqrt{\frac{g}{d_c}} \right)^{0.485} \quad \textit{for steep chutes} \tag{1}$$

where w is the instantaneous width, g is the gravity acceleration, t is the time since the apparition of the surface feature, and the normalised correlation coefficient is 0.80. Eq. (1) is shown and compared to the data in Fig. 4B. The data presented some scatter, which reflected upon the turbulent nature of the interactions between large-scale coherent structures and the free surface, immediately upstream of the inception region (Toro et al., 2017, Chanson, 2022).

The surface scar features were linked to some violent upwelling of large-scale elongated coherent structures. At the same time as the surface breaking took place, some upward stretching of the scar feature took place, with violent air–water processes including air entrapment and air–water fluid expulsion. While the upwelling continued, the violent surface breaking led to the formation of elongated air–water surface features (Fig. 4A). The growth of the elongated air–water surface features yielded the complete aeration of the whole free-surface, i.e. the self-aerated flow region downstream of the inception region. The air–-water surface features presented a variety of elongated shapes in prototype chutes with an aspect ratio, i.e. ratio of length to width, typically greater than 2 to 5 as observed Hinze, Paradise, Somerset and Wivenhoe Dams, Australia (Present study), as well as at Pedrogao Dam, Portugal (Matos and Meireles, 2014) and at Aviemore Dam, New Zealand (Keller, 1972, Cain, 1978). In laboratory, the same air–water surface features presented a ratio of length to width equal about to unity in average, as shown in Fig. 4C. The contrast between prototype and laboratory data hints that some laboratory results in self-aerated flows might not be extrapolated to full-scale prototype spillways without some intrinsic limitations and potential scale effects, already discussed elsewhere (Wood, 1985, Chanson, 1995, Zhang and Chanson, 2017).

(A) Paradise Dam spillway for Q = 2,316 m$^3$/s and Re = 2.9×10$^7$ - Top: approach flow conditions; Bottom: steep spillway chute flow

(B) Hinze Dam spillway for Q = 202 m$^3$/s and Re = 6.7×10$^7$

**Fig. 3.** Self-aeration at prototype spillways during major flood operation - All photographs are high shutter speed with exposure time less than 1 ms.

(C) Chinchilla weir for Q = 121 m$^3$/s and Re = 2.3×10$^6$ (at the crest)

**Fig. 3.** (*continued*).

### 3.2. Inception region

For design engineers, the flow conditions at and location of the inception region of self-aeration are basic design requirements to model the gradually-varied self-aerated flow region (Wood, 1985,1991, Chanson, 1993, Matos, 2000). For all overflows, the prototype data are presented in Fig. 5A, as the dimensionless location of the inception region $L_I/d_c$ as function of the Reynolds number Re. In Fig. 5A, the present data are compared to earlier prototype data. Despite differences in designs, i.e. smooth versus stepped chutes and flat versus steep slopes, all the prototype data were relatively closely correlated as:

$$\frac{L_I}{d_c} = 9 + \frac{4.65 \times 10^5}{\mathrm{Re}^{0.7}} \tag{2}$$

where $L_I$ is the mean position of inception region of free-surface aeration and measured from the chute crest and the normalised correlation coefficient was 0.96. Eq. (2) is compared to the prototype data in Fig. 5A, and the results showed a lower limit $L_I/d_c$ towards 9 for very large Reynolds numbers, i.e. $\mathrm{Re} > 10^8$, irrespective of the chute type and invert slope. The data trend (Fig. 5A) implies potential scale effects in

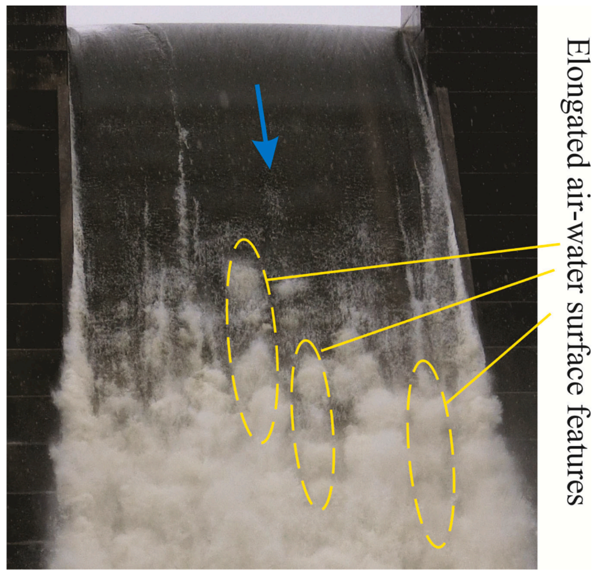


(A) Elongated air-water surface features in the inception region at the Hinze Dam spillway for $Q = 111$ m$^3$/s and Re = 4,5×10$^7$ (shutter speed: 1/1,000 s)

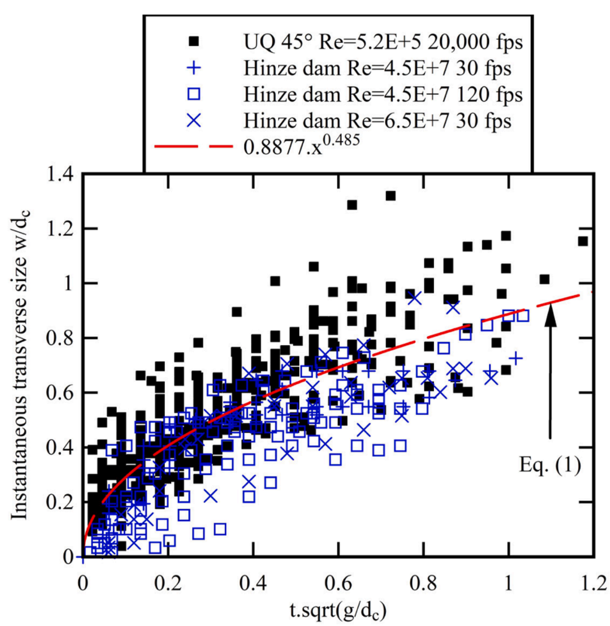


(B) Dimensionless time variation of transverse length of individual surface scars immediately upstream of the inception region in prototype and laboratory chute spillways

**Fig. 4.** Air-water surface features in the inception region on steep-slope chutes (Table 2).

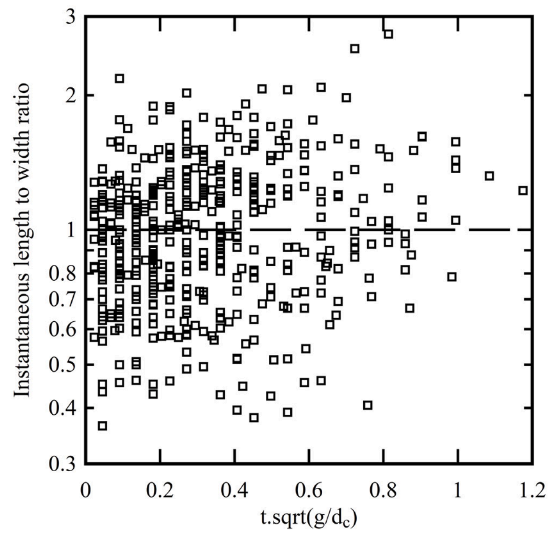


(C) Dimensionless time variations of length to width aspect ratio of individual air-water surface features in laboratory

**Fig. 4.** (*continued*).

**Table 2**
Observations of individual air–water surface features in the inception region of steep spillway chutes (Present study).

| Spillway | Design | θ (°) | Q ($m^3/s$) | q ($m^2/s$) | Re | Aspect ratio $B/d_c$ | Camera frame rate |
|---|---|---|---|---|---|---|---|
| Hinze dam | Stepped (h = 1.5 m) | 51.3 | 140 | 11.4 | $4.5 \times 10^7$ | 5.16 | 30 fps |
| | | | 140 | 11.4 | $4.5 \times 10^7$ | 5.16 | 120 fps |
| | | | 202 | 16.5 | $6.5 \times 10^7$ | 4.04 | 30 fps |
| Laboratory (UQ) | Stepped (h = 0.10 m) | 45.0 | 0.13 | 0.13 | $5.2 \times 10^5$ | 8.21 | 20,000 fps |

terms of the location of the inception region, when extrapolating observations obtained for $Re < 2 \times 10^7$ to larger Reynolds numbers. Eq. (2) differs from historical developments which were derived in terms of a Froude number scaling (Keller and Rastogi, 1975, Wood et al., 1983). Instead, Eq. (2) incorporates the Reynolds number, following boundary layer development theories (Schlichting 1979, Schetz 1993, Chanson, 2014). Further, the range of applications of Eq. (2) covers a broad range of prototype flow conditions for $2 \times 10^6 < Re < 1 \times 10^8$.

The data in terms of dimensionless flow depth $d_I/d_c$ in the inception region are shown in Fig. 5B. The water depth data were obtained from series of high-resolution dSLR photographs (12 Mpx to 24 Mpx) and detailed postconstruction plans. Standard uncertainties of less than 10 mm and 2–5 pixels were assumed for the ground reference point and image coordinates. The corresponding physical photographic uncertainty typically ranged between 0.005 m and 0.015 m per pixel. Despite some scatter, the prototype observations indicated smaller water depths at inception on smooth chute spillways, compared to stepped spillways. The difference was linked in different boundary layer growth rates, between friction-dominated smooth chute flows and form drag-dominated stepped spillway flows. Although some difference is seen between stepped chute data, it may be stressed the high accuracy of the Hinze Dam data set, owing to the excellent and unique physical and optical access and accurate ground reference points (Chanson, 2022).

### 3.3. Surface velocity field

At two prototype spillways, the surface velocity field was derived from an optical technique (OF). The data showed a streamwise distribution with increasing longitudinal surface velocity with decreasing vertical invert elevation at both Hinze Dam and Chinchilla Weir (Chanson, 2022, Chanson and Apelt, 2023). On both chutes, the longitudinal surface velocity maps presented regions of higher velocities and areas of lower velocities, at a given vertical elevation (Fig. 6A). The findings invalidated the "traditional" assumption of two-dimensional flow on spillway chutes and implied a three-dimensional velocity field. The standard deviations of streamwise and transverse surface velocity showed large streamwise surface turbulence and much smaller transverse turbulent intensity. The dimensionless longitudinal turbulence intensity was of the order of magnitude about: $v_s'/V_s \sim 100\,\%$ to $150\,\%$ at both chute spillways, with $V_s$ the time-averaged streamwise surface velocity component and $v_s'$ the standard deviation of the streamwise surface velocity component (Fig. 6B). The dimensionless velocity fluctuation data were comparable to laboratory observations of surface velocity fluctuations in large-size laboratory chutes, obtained with total pressure probe, dual-tip phase detection probe and optical flow with ultra-high-speed video camera (e.g. Zhang and Chanson, 2016, Arosquipa Nina et al., 2022). Fig. 6B presents a comparison of prototype and laboratory observations, with similar trend and order of magnitude for all data sets. In Fig. 6B, the phase-detection probe data were recorded at $y = Y_{90}$ where the void fraction was 90 %. For the prototype data (Hinze Dam, Chinchilla Weir), it is believed that the natural lighting would likely contribute to the greater uniform data trend, seen in Fig. 6B. Indeed, one cannot stress the importance of lighting conditions when using optical techniques (Chanson and Shi, 2022, Bung, 2023). Altogether, these high turbulence levels were caused by a combination of free-surface turbulence and free-surface fluctuations in the direction normal to the invert, as well as instationary hydrodynamic instabilities (Felder and Chanson, 2014, Chanson, 2022).

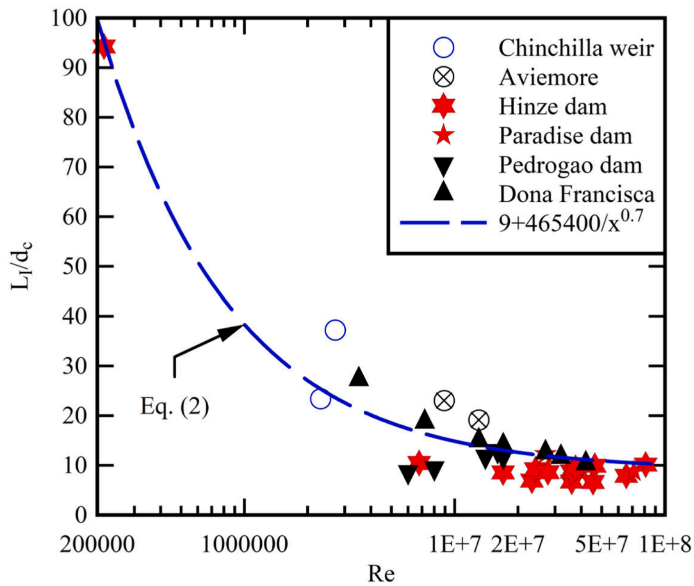


(A) Longitudinal location of the inception region including a comparison with Equation (2)

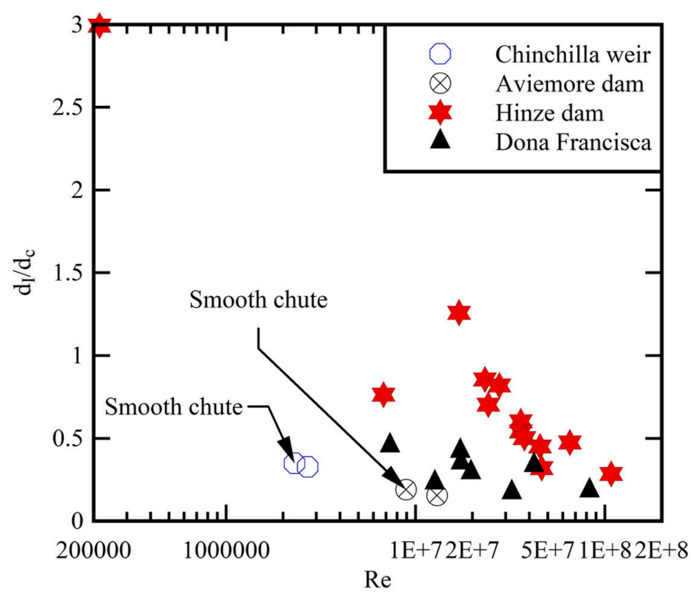


(B) Water depth in the inception region

**Fig. 5.** Dimensionless location $L_I/d_c$ of and water depth $d_I/d_c$ at the inception region on prototype spillway chutes as functions of the Reynolds number Re - Comparison between prototype smooth chute data (Aviemore dam, Chinchilla weir) and prototype stepped chute data (Hinze dam, Paradise dam, Pedrogao dam, Dona Francisca dam) (Present study, Cain and Wood, 1981, Chanson et al., 2015).

Basically, the surface velocity and turbulence intensity data recorded in prototype spillways demonstrated a two-dimensional surface velocity field, implying a strong three-dimensionality of the self-aerated spillway chute flows. The supercritical chute flows entering the downstream stilling basin would include some regions of kinetic energy peaks, and the finding has some direct implication into the safe design of downstream energy dissipators.

## 4. Concluding outcomes

Today, the planet Earth is experiencing an increasing number of extreme water events, including with droughts and floods (Jonkman, 2005, Rojas et al., 2013). Both flood protection and water security are becoming vital to mankind. Water reservoirs can deliver both (Novak et al., 1996,2007) and the dams must be equipped with a spillway structure to pass safely the flood waters above, below, beneath or beside the dam wall. Despite the numerous hydraulic design manuals, what do we know really about prototype spillway operation during major floods, beyond limited visual qualitative observations and physical modelling in facilities drastically smaller than the full-scale prototype spillways? Not much really! Detailed quantitative measurements in prototype spillway overflow are rare, especially during very large floods. One cannot stress enough the importance of prototype field measurements because they apply to the full-scale infrastructure. Despite a sizeable number of

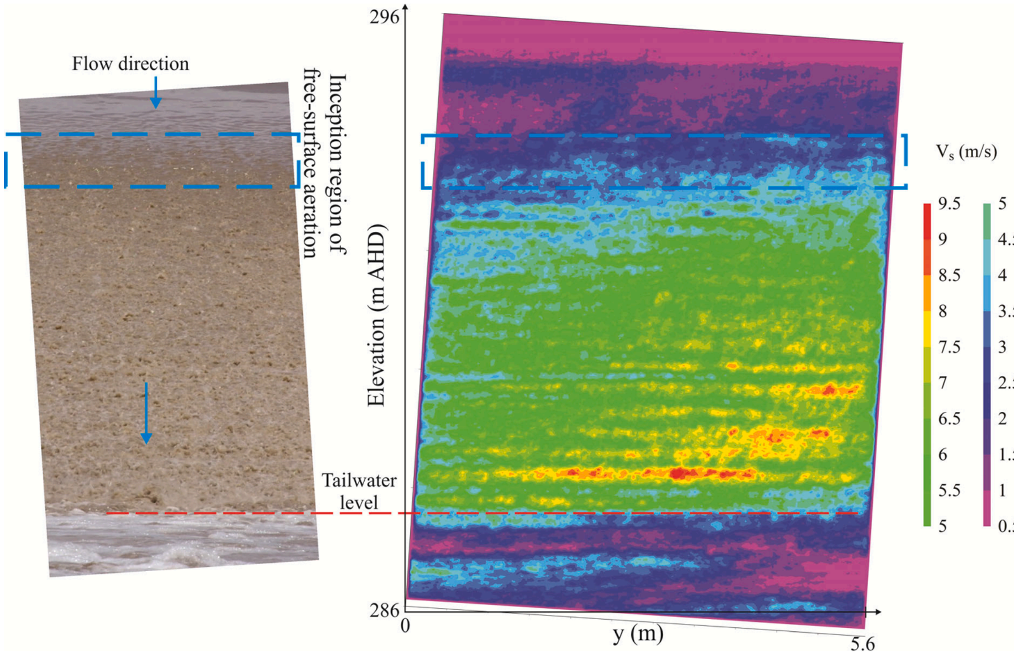


(A) Contour map of longitudinal surface velocity $V_s$ at Chinchilla Weir (left spillway bay) for $Q = 121\ m^3/s$ and $Re = 2.3\times10^6$ (at spillway crest)

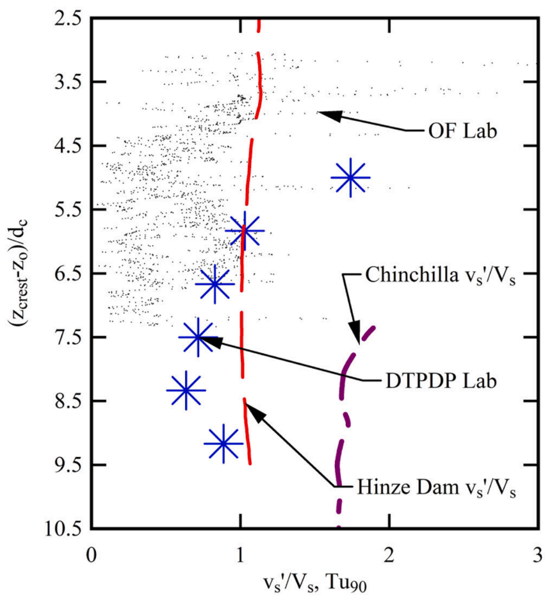


(B) Dimensionless vertical variations of longitudinal turbulence intensity $v_s'/V_s$ at Chinchilla weir ($Q = 144\ m^3/s$, $Re = 2.7\times10^6$) at Hinze Dam ($Q = = 140\ m^3/s$, $Re = 4.5\times10^7$) and in laboratory ($Q = 0.13\ m^3/s$, $Re = 5.2\times10^5$) - DTPTP = dual-tip phase detection probe data at $y = Y_{90}$ where the void fraction was 90%; OF = optical flow - Note that the critical flow conditions ($d_c$, $V_c$) are calculated at the spillway crest.

**Fig. 6.** Surface velocity measurements at prototype spillways during major flood operation.

intrinsic difficulties, the field measurements represent the ultimate "truth". In plain terms, quantitative prototype data constitute a fundamental requirement for the proper validation of successful hydraulic designs as well as the validation of experimental, theoretical and computational modelling.

In the last few decades, a number of recent developments in physical and optical observations delivered a few prototype spillway tests (Cain and Wood, 1981, Falvey, 1982, Volkart and Rutschmann, 1984, Hohermuth et al., 2021, Bai et al. 2022). While controlled prototype tests are very valuable to provide documented answers to many design questions, the test flow conditions are usually idealised. That is, the full-scale tests are typically conducted for short durations, with water discharges significantly smaller than design flow conditions, with smooth inflow, and with low debris and sediment contents. Such conditions differ from major flood events, and a senior dam engineer warned of the "*fallacy*" behind full-scale testing (Elder 1984b). Today, there remains a critical need to fill the knowledge gap in detailed prototype observations during major floods and natural disaster events.

Many variables are uncontrolled during prototype hydraulic structure overflows, in comparison to laboratory experiments. A sizeable amount of scientific discussions has been centered on the physical modelling in laboratory and scale effects affecting the extrapolation of laboratory results (Kobus, 1984, Chanson, 2009, Novak et al., 2010). In contrast, detailed reports on the hydraulic operation of large dams' spillways during major floods are rare, unless there are accidents, incidents or failure. A notable exception was a special seminar held in 2001 (Burgi and Gao, 2001). Thus, an expert hydraulic engineer should ask: how large the Reynolds number of a prototype flow needs to be? Let us remember that the flow conditions for a few seminal prototype data sets corresponded to Reynolds numbers Re about $10^6$ to $3 \times 10^6$: e.g., at the Aviemore dam spillway (Cain and Wood, 1981), La Grande Dixence spillway chute (Volkart and Rutschmann, 1984) and Pangzhuang gate (Bai et al., 2021). The flow conditions of these data sets were one to two orders of magnitude lower than the design flow conditions of many large dam spillway systems, including the Hinze Dam and Paradise Dam spillway chutes. In this context, the current contribution encompasses prototype spillway data collected at large Reynolds numbers up to $1.1 \times 10^8$ and discharges in excess of $100\,m^3/s$. This constitutes an original attempt to develop the state-of-the art expertise in air–water flows in spillway flow and to expand our knowledge in ultra-high-Reynolds number free-surface flows.

## Declaration of competing interest

The authors declare the following financial interests/personal relationships which may be considered as potential competing interests: In line with recommendations of the International Committee on Publication Ethics (COPE) and the Office of the Commonwealth Ombudsman (Australia), Hubert Chanson declares a major conflict of interest with Matthias Kramer (University of New South Wales, Canberra) and Stefan Felder (University of New South Wales). Matthias Kramer and Stefan Felder made false allegations of plagiarism against Professor Chanson, his student and his research fellow. The allegations were investigated independently and found un-substantiated by very senior scholars.

## Acknowledgments

The author thanks many people for their assistance during the field observations (Ms Ya-Hui Chou, André Chanson, Bernard Chanson) and data processing (Dr Rui Shi, Prof. Colin J. Apelt, Barton Maher, Leigh Cook and Tobias Burwood) as well as several agencies (Seqwater, Sunwater, Western Downs Regional Council). He also acknowledges data provided by Prof. Jorge Matos and Mr Rui Yang.

## References

Anwar, H.O., 1994. Self-aerated flows on chutes and spillways - discussion. J. Hydraul. Eng., ASCE 120 (6), 778–779.

Arosquipa Nina, Y, Shi, R., Wüthrich, D., and Chanson, H. (2022). "Intrusive and Non-Intrusive Two-Phase Air-Water Measurements on Stepped Spillways: a Physical Study." *Experimental Thermal and Fluid Science*, Vol. 131, Paper 110545, 22 pages, 4 movies and a digital appendix (6 pages) (https://doi.org/10.1016/j.expthermflusci.2021.110545).

Bai, Z., Bai, R., Tang, R., Wang, H., Liu, S., 2021. Case Study of Prototype Hydraulic Jump on Slope: Air Entrainment and Free-Surface Measurement. J. Hydraul. Eng, ASCE 147 (9), 12. https://doi.org/10.1061/(ASCE)HY.1943-7900.0001916. Paper 05021007.

Bung, D.B., 2023. Imaging Techniques for Investigation of Free-surface Flows in Hydraulic Laboratories. Habilitation Thesis. University of Wuppertal, Germany, p. 242.

Bung, D.B., Valero, D., 2016. Optical flow estimation in aerated flows. J. Hydraul. Res., IAHR 54 (5), 575–580. https://doi.org/10.1080/00221686.2016.1173600.

P.H. Burgi J. Gao " Key Hydraulic Issues of Huge Water Projects." Proc. 29th IAHR Congress, Beijing, China, Special Seminar SS2, Tsinghua University Press, Beijing, Guifen Li Editor 2001 130.

Cain, P., Wood, I.R., 1981. Measurements of self-aerated flow on a spillway. J. Hydraul. Div., ASCE 107 (HY11), 1425–1444.

Cain, P. (1978). "Measurements within Self-Aerated Flow on a Large Spillway." *Ph.D. Thesis*, Ref. 78-18, Dept. of Civil Engrg., Univ. of Canterbury, Christchurch, New Zealand.

Cassidy, J.J., Elder, R.A., 1984. "Spillways of high dams." in "developments in hydraulic engineering." *elsevier*, London, P. NOVAK Editor, Chapter 4, 159–182.

Chanson, H., 1993. Self-aerated flows on chutes and spillways. J. Hydraul. Eng., ASCE 119 (2), 220–243. https://doi.org/10.1061/(ASCE)0733-9429(1993)119:2(220).

Chanson, H., 1995. "Air bubble diffusion in supercritical Open Channel flow." *proc. 12th australasian fluid mechanics conference AFMC*, Sydney, Australia, R.W. Bilger Editor 2, 707–710.

Chanson, H., 1997. Air bubble entrainment in open channels. flow structure and bubble size distributions. Int. J. Multiph. Flow 23 (1), 193–203. https://doi.org/10.1016/S0301-9322(96)00063-8.

Chanson, H., 2009. Turbulent air-water flows in hydraulic structures: dynamic Similarity and scale effects. Environ. Fluid Mech. 9 (2), 125–142. https://doi.org/10.1007/s10652-008-9078-3.

Chanson, H., 2013. "Interactions between a Developing Boundary Layer and the Free-Surface on a Stepped Spillway: Hinze Dam Spillway Operation in January 2013." {https://espace.library.uq.edu.au/view/UQ:301643}.

Chanson, H., 2014. Applied hydrodynamics: an introduction. CRC Press, Taylor & Francis Group, Leiden, The Netherlands, 448 pages & 21 video movies.

H. Chanson R. Shi "Optical measurements in dam spillways during major flood events: a down-to-earth review of pros and cons." Proceedings of 30th Hydrology and Water Resources Symposium HWRS2022, Brisbane, Australia, 30 November-2 December, Published by Engineers Australia, Brisbane, Australia, Paper 08 2022 53 63.

Chanson, H., Apelt, C.J., 2022. In: Surface Velocities and Free-Surface Aeration in a Converging Smooth Chute during a Major Flood Event. Utah State University, Logan, USA, pp. 180–189. https://doi.org/10.26077/11eb-458d.

Chanson, H., Apelt, C.J., 2023. Environmental fluid mechanics of minimum energy loss weirs: hydrodynamics and self-aeration at Chinchilla MEL weir during the november-december 2021 flood event. Environ. Fluid Mech. 23 (3), 633–659. https://doi.org/10.1007/s10652-023-09926-0.

Chanson, H., Bung, D., and Matos, J. (2015). "Stepped spillways and cascades." in "Energy Dissipation in Hydraulic Structures." *IAHR Monograph*, CRC Press, Taylor & Francis Group, Leiden, The Netherlands, H. Chanson Editor, pp. 45-64.

Chanson, H., 2022. Stepped Spillway Prototype Operation and Air Entrainment: Toward a Better Understanding of the Mechanisms Leading to Air Entrainment in Skimming Flows. J. Hydraul. Eng. ASCE 148 (11), 17. https://doi.org/10.1061/(ASCE)HY.1943-7900.0002015. Paper 05022004.

Chanson, H. (2023). "Self-aeration in free-surface flows at high Reynolds number (2.6E+6 - 1.1E+8)." *Proc. 40th IAHR World Congress*, 21-25 August, Vienna, Austria, 10 pages.

Elder, R.A., 1984. "Scaling is Vital to the Practicing Engineer.". In: Kobus, H. (Ed.), General Lecture, p. 3. Paper 0.1.

Ervine, D.A., Falvey, H.T., 1987. Behaviour of turbulent water jets in the atmosphere and in plunge pools. Proceedings of the Institution Civil Engineers.

Falvey, H.T. (1982). "Predicting Cavitation in Tunnel Spillways." *International Water Power and Dam Construction*, Vol. 34, No. 8, Aug., pp- 13-15.

Felder, S., Chanson, H., 2014. Triple decomposition technique in air-water flows: application to Instationary flows on a stepped spillway. Int. J. Multiph. Flow 58, 139–153. https://doi.org/10.1016/j.ijmultiphaseflow.2013.09.006. & 3 videos.

Hino, M., 1961. "A theory of the mechanism of self-aerated flow on steep slope channels. applications of the statistical theory of turbulence." *technical report C-6101*, technical laboratory, Central Research Institute of Electric Power Industry. Japan 42, pages.

Hohermuth, B., Boes, R., Felder, S., 2021. High-velocity air-water flow measurements in a prototype tunnel chute: scaling of void Fraction and Interfacial velocity. *J. Hydraul. Eng.*, ASCE Vol. 147, No. 11, Paper 04021044, 11 pages.

ICOLD (1984). "World Register of Dams - Registre Mondial des barrages - ICOLD." *International Commission on Large Dams*, Paris, France, 753 pages.

Jonkman, S.N., 2005. Global perspectives on loss of human life caused by floods. Nat. Hazards 34, 151–175.

Keller, R.J., Rastogi, A.K., 1975. Prediction of flow development on spillways. J. Hydraul. Div., ASCE 101 (HY9), 1171–1184.

Keller, R.J. (1972). "Field Measurement of Self-Aerated High Speed Open Channel Flow." *Ph.D. thesis*, Dept. of Civil Eng., Univ. of Canterbury, New Zealand.

Kobus, H. (1984). "Scale Effects in Modelling Hydraulic Structures." *Institut fur Wasserbau, Universitat Stuttgart*, IAHR International Symposium on Scale Effects in Modelling Hydraulic Structures, IAHR, Esslingen, Germany.

Kolkman, P.A., 1984. Considerations about the Accuracy of Discharge relations of hydraulic structures and the use of scale models for their calibration. IAHR, Esslingen, Germany, H. KOBUS.

Levi, E., 1965. Longitudinal streaking in liquid currents. J. Hydraul. Res., IAHR 3 (2), 25–39.

Levi, E., 1967. "Macroturbulence produced by vortex breakdown in high velocity flows." *proc. 12th IAHR congress*, Colorado, USA, vol. 2. Paper B7, 54–60.

J. Matos I. Meireles "Hydraulics of stepped weirs and dam spillways: engineering challenges, labyrinths of research." Proceedings of the 5th IAHR International Symposium on Hydraulic Structures (ISHS2014), 25-27 June 2014, The University of Queensland, Brisbane, Australia, H. Chanson and L. Toombes Editors 2014 30 10.14264/uql.2014.11.

Matos, J. (2000). "Hydraulic Design of Stepped Spillways over RCC Dams." *Intl Workshop on Hydraulics of Stepped Spillways*, Zürich, Switzerland, H.E. Minor & W.H. Hager Editors, Balkema Publ., pp. 187-194.

Michels, V., Lovely, M., 1953. "Some prototype observations of air entrained flow." *proc*, 5th IAHR Congress,. IAHR-ASCE, Minneapolis, USA, pp. 403–414.

Novak, P., Moffat, A.I.B., Nalluri, C., and Narayanan, R. (2007). "Hydraulic Structures." Taylor & Francis, London, UK, 4th edition, 700 pages.

Novak, P., Guinot, V., Jeffrey, A., and Reeve, D.E. (2010). "Hydraulic Modelling - an Introduction." *CRC Press*, Taylor & Francis, London, UK, 599 pages.

Novak, P., Moffat, A.I.B., Nalluri, C., Narayanan, R., 1996. Hydraulic structures, 2nd edition,. E&FN Spon, London, UK, p. 599 pages..

Rao, N.S.G., Rajaratnam, N., 1961. On the inception of air entrainment in Open Channel flows. In: Proc. 9th IAHR Congress, pp. 9–12.

Rojas, R., Feyen, L., Watkiss, P., 2013. Climate change and river floods in the European Union: socio-economic consequences and the costs and benefits of adaptation. Glob Environ Change 23, 1737–1751.

Toro, J.P., Bombardelli, F.A., Paik, J., 2017. Detached Eddy simulation of the nonaerated skimming flow over a stepped spillway. *J. Hydraul. Eng.*, ASCE 143 (9), 14. Paper 04017032.

Turnbull, J.D., and McKay, G.R. (1974). "The Design and Construction of Chinchilla Weir - Condamine River Queensland." *Proc. 5th Australasian Conference on Hydraulics and Fluid Mechanics*, Christchurch, New Zealand, Vol. II, pp. 1-8.

USBR (1965). "Design of Small Dams." *Bureau of Reclamation*, Denver CO, USA, US Department of the Interior, 1st edition, 3rd printing.

Volkart, P., Rutschmann, P., 1984. Rapid flow in spillway chutes with and without deflectors - a model-prototype Comparison. IAHR, Esslingen, Germany, H. KOBUS.

Wood, I.R., Ackers, P., Loveless, J., 1983. General method for critical point on spillways. *J. Hydraul. Eng.*, ASCE 109 (2), 308–312.

I.R. Wood (1985). "Air Water Flows." *Proc. 21st IAHR Congress*, Melbourne, Australia, Keynote address, pp. 18-29.

Wood, I.R. (1991). "Air Entrainment in Free-Surface Flows." *IAHR Hydraulic Structures Design Manual No. 4*, Hydraulic Design Considerations, Balkema Publ., Rotterdam, The Netherlands, 149 pages.

Zabaleta, F., and Bombardelli, F.A. (2020). "Eddy-resolving Simulation of Flows over Macroroughness." *Proceedings of RiverFlow2020*, CRC Press, Uijttewaal et al. Editors, pp. 1293-1299.

Zhang, G., Chanson, H., 2016. Interactions between free-surface aeration and Total pressure on a stepped chute. Exp. Therm Fluid Sci. 74, 368–381. https://doi.org/10.1016/j.expthermflusci.2015.12.011.

Zhang, G., Chanson, H., 2017. Self-aeration in the rapidly- and gradually-varying flow regions of steep smooth and stepped spillways. Environ. Fluid Mech. 17 (1), 27–46. https://doi.org/10.1007/s10652-015-9442-z.

Zhang, G., Chanson, H., 2019. Application of optical flow methods to aerated skimming flows above Triangular and trapezoidal step cavities. *J. Hydraul. Res.*, IAHR 57 (4), 488–497. https://doi.org/10.1080/00221686.2018.1489900.